Universal Power-Hardware-in-the-Loop Simulator for BLDCM and PMSM

Xu Jiaqun*, Xing Meili, and Zhang Hongqiang

Faulty of Information Technology, Beijing University of Technology, Beijing 100124, China

To improve the test efficiency and reduce the test cost, this paper presents a design method of universal power-hardware-in-the-loop (PHIL) simulator for brushless DC motor (BLDCM) and permanent magnet synchronous motor (PMSM). The actual stator winding is simulated by the power-level current source in the simulator, thus, the electric power can be interacted between the simulator and the motor driver. By the method of bilinear transform and inverse Z-transform, the line voltage based numerical models of the virtual motors are derived. Moreover, the relationship between the line voltage and phase current of the virtual motors is analyzed, which is used to calculate the phase current commands in the numerical models. Furthermore, the universal PHIL simulator is implemented and the real-time simulation is performed, and then the offline simulation with MATLAB software and the actual motor test are also performed to verify the simulator results. The simulation and experimental results show that both PMSM and BLDCM can be simulated accurately at the power level without changing any hardware of the motor driver and the simulator.

Keywords : Power-hardware-in-the-loop, simulator, brushless DC motor, permanent magnet synchronous motor, numerical model, real-time simulation

1. Introduction

With advantages of high efficiency, high torque density and high power density, permanent magnet synchronous motor (PMSM) and brushless DC motor (BLDCM) are widely used [1, 2]. However, the motor driver test is very troublesome. The well-known approach is using the actual motor and the mechanical test bench, which is obviously a time-consuming and high cost process.

To solve the problem, it is necessary to replace the actual motor and the mechanical test bench with the hardware-in-the-loop (HIL) simulator, and there are two kinds of HIL simulators used in motors.

One is the signal-hardware-in-the-loop (SHIL) simulator, which is in wide use for its flexible test, short development cycle and low cost [3-5]. However, there is no electric power transfer between the motor driver and the SHIL simulator. Thus, as an important part, the power stage of the motor driver cannot be tested by the SHIL simulator.

The other is the power-hardware-in-the-loop (PHIL) simulator, which is the extension of the SHIL simulator.

The actual motor winding is simulated by the special power stage in the PHIL simulator, then both the electric power and signals can be interacted between the PHIL simulator and the actual motor driver [6, 7]. Therefore, all parts of the motor driver, including the power stage, can be tested based on the PHIL simulator. As the virtual motor, the PHIL simulator is a flexible and convenient device to test the motor driver at the power level.

Nevertheless, little work has been done on the PHIL simulator for BLDCM and PMSM. In [6], the structure of the BLDCM driver under test needs to be modified to fit for the PHIL simulator, however, that is not allowed in most cases. Moreover, the neutral point of the motor driver is often not available, which means that the conventional phase voltage based mathematical model is not applicable for the PHIL simulator. In addition, the transient process of the BLDCM simulator is rarely mentioned. Recently, it has been found that the PMSM HIL simulator are still at the signal level [2-4]. It is thus clear that the problems about the PHIL simulator for BLDCM and PMSM have never been satisfactorily solved.

This paper proposes a design method of universal PHIL simulator for both BLDCM and PMSM. The line voltage based numerical models for the two kinds of motors are derived, and the simulator structure and control are also

presented. The simulator is implemented, and the real-time simulation for BLDCM and PMSM at the power level is realized without changing any hardware structure of the motor driver. The effectiveness of the universal PHIL simulator is validated by simulation and experimental results.

2. Universal Simulator Numerical Models

The voltage equation of BLDCM is expressed as:

$$\begin{bmatrix} u_a \\ u_b \\ u_c \end{bmatrix} = \begin{bmatrix} R & 0 & 0 \\ 0 & R & 0 \\ 0 & 0 & R \end{bmatrix}\begin{bmatrix} i_a \\ i_b \\ i_c \end{bmatrix} + \begin{bmatrix} L & 0 & 0 \\ 0 & L & 0 \\ 0 & 0 & L \end{bmatrix} \cdot \frac{d}{dt}\begin{bmatrix} i_a \\ i_b \\ i_c \end{bmatrix} + \begin{bmatrix} e_a \\ e_b \\ e_c \end{bmatrix} \qquad (1)$$

Where u_a, u_b, and u_c, are, respectively, the winding voltages of the phase a, b, and c; e_a, e_b, and e_c are, respectively, the winding back EMFs of the phase a, b, and c; i_a, i_b, and i_c are, respectively, the winding currents of the phase a, b, and c; R and L are, respectively, the winding resistance and inductance.

The voltage and current equations of surface-mounted PMSM are expressed as:

$$\begin{cases} u_d = Ri_d + L\,di_d/dt - \omega Li_q \\ u_q = Ri_q + L\,di_q/dt + \omega Li_d + \omega\lambda \end{cases} \qquad (2)$$

$$\begin{bmatrix} f_a \\ f_b \\ f_c \end{bmatrix} = \sqrt{\frac{2}{3}}\begin{bmatrix} \cos\theta & -\sin\theta \\ \cos(\theta - 2\pi/3) & -\sin(\theta - 2\pi/3) \\ \cos(\theta + 2\pi/3) & -\sin(\theta + 2\pi/3) \end{bmatrix}\begin{bmatrix} f_d \\ f_q \end{bmatrix} \qquad (3)$$

Where u_d and u_q are the d-axis and q-axis voltage, respectively; i_d and i_q are the d-axis and q-axis current, respectively; ω is the electrical angular frequency; λ is the permanent magnet flux linkage; θ is the rotor angle between the rotor flux direction and the a-axis; f denotes the voltage u or the current i.

The back EMF equations of BLDCM and PMSM can be expressed as follows:

$$\begin{cases} e_a = \lambda p\omega_m \sin\theta = \lambda p\omega_m \phi_a \\ e_b = \lambda p\omega_m \sin(\theta - 2\pi/3) = \lambda p\omega_m \phi_b \\ e_c = \lambda p\omega_m \sin(\theta + 2\pi/3) = \lambda p\omega_m \phi_c \end{cases} \qquad (4)$$

Where p is the number of pole pairs; ω_m is the mechanical angular frequency.

Thus, the differential equations are obtained as below:

$$\begin{cases} di_a/dt = [U_{ab} + U_{ac} - 3Ri_a + \lambda p\omega_m(-2\phi_a + \phi_b + \phi_c)]/3L \\ di_b/dt = [-2U_{ab} + U_{ac} - 3Ri_b + \lambda p\omega_m(\phi_a - 2\phi_b + \phi_c)]/3L \\ di_c/dt = -(di_a/dt + di_b/dt) \end{cases} \qquad (5)$$

Where U_{ab} and U_{ac} are the line-to-line voltage.

The motion equation is as follows:

$$d\omega_m/dt = (T_e - T_f - F \cdot \omega_m - T_m)/J \qquad (6)$$

Where T_e is the electromagnetic torque; J is the rotor inertia; F is the viscous friction; T_m is the mechanical torque; T_f is the static friction torque.

The electromagnetic torque of BLDCM and PMSM are, respectively, as follows:

$$T_e = \lambda p(\phi_a i_a + \phi_b i_b + \phi_c i_c) \qquad (7)$$

$$T_e = \frac{3}{2}p\lambda i_q \qquad (8)$$

The electrical rotor position can be expressed as:

$$d\theta/dt = p\omega_m \qquad (9)$$

Laplace transform is used to equation (5) and (6), we obtain

$$\begin{cases} \dfrac{I_a(s)}{U_{ab}(s) + U_{ac}(s) + \lambda p\omega_m(-2\phi_a + \phi_b + \phi_c)} = \dfrac{1}{3(Ls + R)} \\[4mm] \dfrac{I_b(s)}{-2U_{ab}(s) + U_{ac}(s) + \lambda p\omega_m(\phi_a - 2\phi_b + \phi_c)} = \dfrac{1}{3(Ls + R)} \end{cases} \qquad (10)$$

$$\frac{\Omega(s)}{T_e(s) - T_f(s) - T_m(s)} = \frac{1}{Js + F} \qquad (11)$$

Bilinear transformation is used to equation (10) and (11), we obtain

$$\frac{1}{3(Ls + R)}\Big|_{s=\frac{2}{T}\frac{1-z^{-1}}{1+z^{-1}}} = \frac{\dfrac{T}{3(2L + RT)} + \dfrac{T}{3(2L + RT)}z^{-1}}{1 + \dfrac{RT - 2L}{RT + 2L}z^{-1}} \qquad (12)$$

$$\frac{1}{Js + F}\Big|_{s=\frac{2}{T}\frac{1-z^{-1}}{1+z^{-1}}} = \frac{\dfrac{T}{FT + 2J} + \dfrac{T}{FT + 2J}z^{-1}}{1 + \dfrac{FT - 2J}{FT + 2J}z^{-1}} \qquad (13)$$

Where T is the numerical integration step size.

Next, inverse z-transform is used to obtain the numerical models as follows:

$$i_k = -\frac{RT - 2L}{RT + 2L}i_{k-1} + \frac{T}{3(2L + RT)}u_k + \frac{T}{3(2L + RT)}u_{k-1} \qquad (14)$$

$$\omega_k = -\frac{FT - 2J}{FT + 2J}\omega_{k-1} + \frac{T}{FT + 2J}t_k + \frac{T}{FT + 2J}t_{k-1} \qquad (15)$$

Equation (14) and (15) can be programmed directly in the general processor. The current model and mechanical angular frequency model are same for BLDCM and PMSM, however, the back EMF model and torque model are different.

3. Simulator Structure and Control

Based on the above analysis of numerical models, the universal PHIL simulator structure is presented, which is shown in Fig. 1. The numerical models are realized in the general processor. The rotor angle is obtained either through the simulated hall sensor signals of the virtual BLDCM, or through the simulated resolver excitation and feedback signals of the virtual PMSM. Based on the line voltages U_{AB} and U_{AC} from the motor driver, the virtual winding voltages U_{ab} and U_{ac} can be obtained. The numerical models are used to calculate back EMFs,
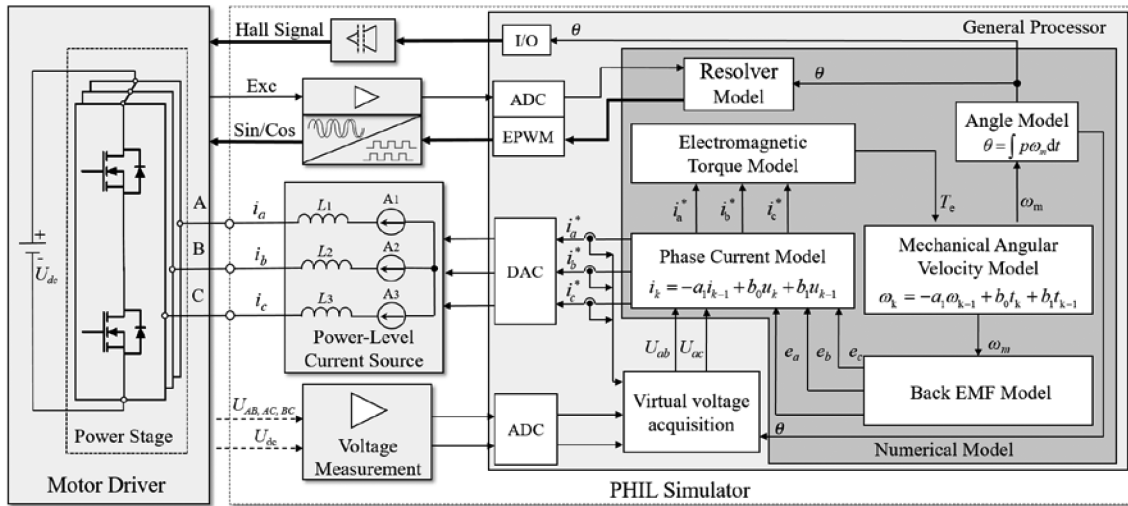
(a)
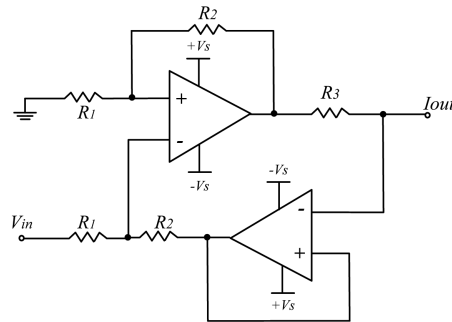
(b)
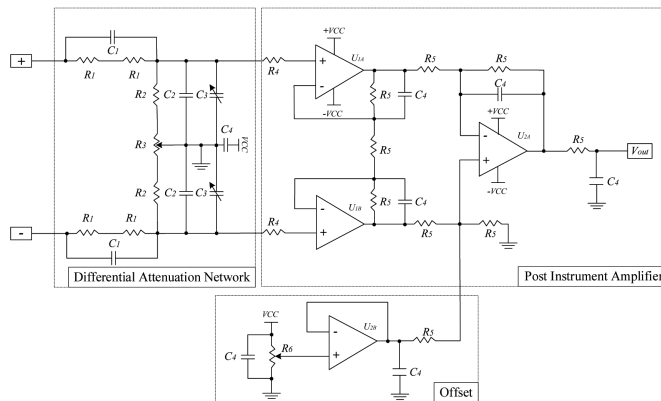
(c)

Fig. 1. Structure of universal PHIL simulator. (a) PHIL structure. (b) Power-level current source. (c) Analog front end for line voltage measurement.

electromagnetic torque, rotor angle, phase current commands i_a^*, i_b^* and i_c^*, and mechanical angular frequency. Moreover, the phase current commands are converted into the actual phase currents through the power-level current source.

A linear mode power operational amplifier based current source shown in Fig. 1(b) is used as the power stage of the PHIL simulator, which plays a role in exchanging real electric power between the motor driver and the PHIL simulator. V_{in} is the input signal connected to the phase current commands i_a^*, i_b^*, i_c^*, and I_{out} is the output terminal connected to the BLDCM driver, then the transfer function about the voltage controlled current source can be expressed as:

$$I_{out} = \frac{V_{in}}{R_s} \frac{R_f}{R_i} \tag{16}$$

To measure the PWM line voltage from the motor driver with low distortion and high precision, the analog front end (AFE) shown in Fig. 1(c) is presented. The AFE mainly consists of the differential attenuation network and the instrument amplifier, which can provide the characteristics of high bandwidth, high slew rate and high input impedance.

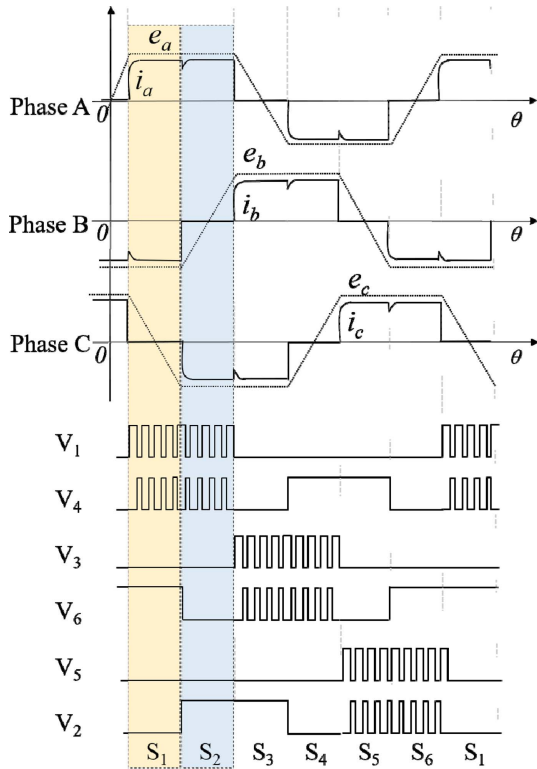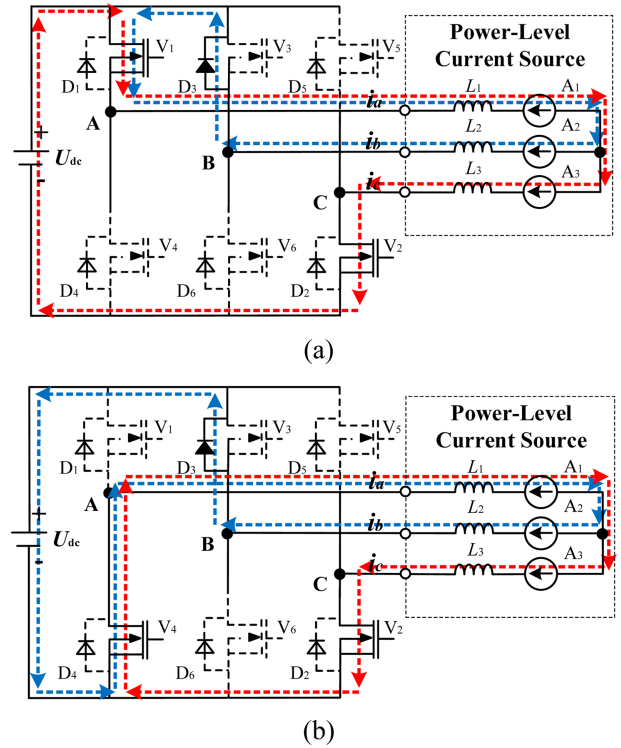When BLDCM operates in the six-step commutation

(a)

(b)

Fig. 3. (Color online) Current loops of BLDCM simulator in commutation process from interval S_1 to S_2. (a) V_1 on. (b) V_1 off.

mode, as shown in Fig. 2, there are six two-phase conduction intervals from S_1 to S_6 in one control period. The intervals S_1 and S_2 are chosen as an example to analyze the relationship between current and voltage in the simulator.

In the transient commutation process of BLDCM from interval S_1 to S_2, there are two modes about switch V_1 in one PWM period. In Fig. 3(a), when switch V_1 is on, the current loops are $A_1 \rightarrow A_2 \rightarrow L_2 \rightarrow D_3 \rightarrow V_1 \rightarrow L_1 \rightarrow A_1$ and $U_{dc} \rightarrow V_1 \rightarrow L_1 \rightarrow A_1 \rightarrow A_3 \rightarrow L_3 \rightarrow V_2 \rightarrow U_{dc}$, respectively, and thus, $U_{AB} = -U_D$ and $U_{AC} = U_{dc}$. In Fig. 3(b), when switch V_1 is off, the current loops are $A_1 \rightarrow A_2 \rightarrow L_2 \rightarrow D_3 \rightarrow U_{dc} \rightarrow V_4 \rightarrow L_1 \rightarrow A_1$ and $A_1 \rightarrow A_3 \rightarrow L_3 \rightarrow V_2 \rightarrow V_4 \rightarrow L_1 \rightarrow A_1$, respectively, and thus, $U_{AB} = -U_{dc} - U_D$ and $U_{AC} = 0$.

After the above transient commutation, the current loops of BLDCM simulator in steady state interval S_2 are shown in Fig. 4. In Fig. 4(a), when switch V_1 is on, the current loop is $U_{dc} \rightarrow V_1 \rightarrow L_1 \rightarrow A_1 \rightarrow A_3 \rightarrow L_3 \rightarrow V_2 \rightarrow U_{dc}$. Hence, in this mode, $U_{AB} = 1/2U_{dc}$ and $U_{AC} = U_{dc}$. In Fig. 4(b), when switch V_1 is off, the current loop is $A_1 \rightarrow A_3 \rightarrow L_3 \rightarrow V_2 \rightarrow V_4 \rightarrow L_1 \rightarrow A_1$. Thus, in this mode, $U_{AB} = 0$ and $U_{AC} = 0$.

Based on the above analysis about the intervals S_1 and S_2, the relationship between phase current and line voltage in all six intervals can be obtained, which will be
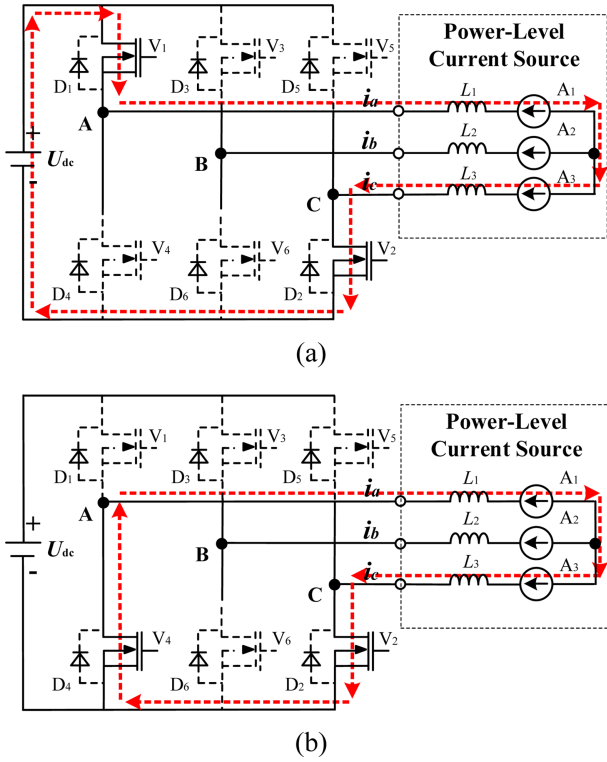

Fig. 2. (Color online) Back EMFs, current and switching sequences of BLDCM in six-step commutation mode.

Fig. 4. (Color online) Current loops of BLDCM simulator in steady state interval S_2. (a) V_1 on. (b) V_1 off.

used to calculate the phase current commands in the BLDCM numerical model.

When PMSM operates in the vector control mode, as shown in Fig. 5, there are six nonzero voltage space vectors from U_1 to U_6. The two vectors U_4 and U_6 are chosen as an example to analyze the relationship between
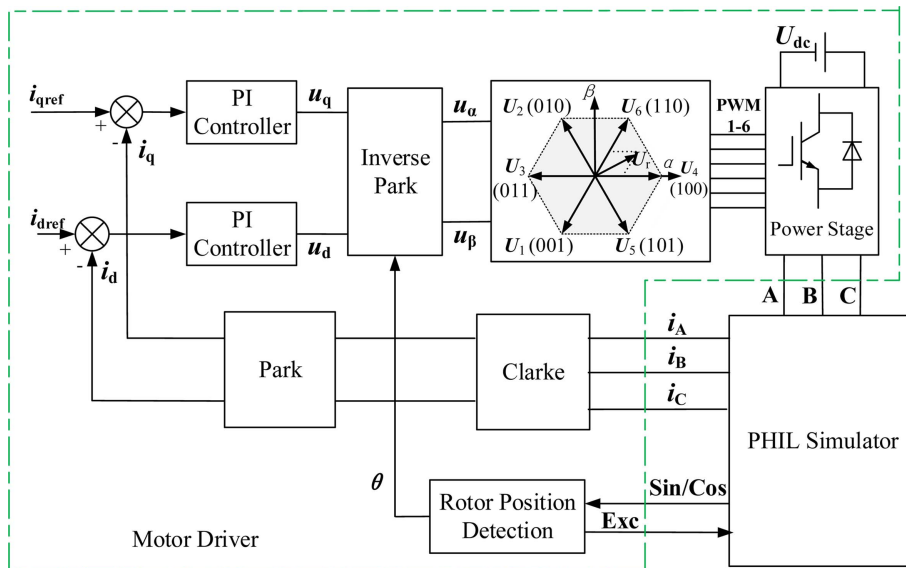
current and voltage in the simulator.

Fig. 6 shows the current loops of PMSM simulator from vector U_4 to U_6. It can be seen from Fig. 6(a) that in the transient state process, the current loops are $U_{dc} \rightarrow V_1 \rightarrow L_1 \rightarrow A_1 \rightarrow A_3 \rightarrow L_3 \rightarrow V_2 \rightarrow U_{dc}$ and $U_{dc} \rightarrow V_3 \rightarrow L_2 \rightarrow A_2 \rightarrow A_3 \rightarrow L_3 \rightarrow V_2 \rightarrow U_{dc}$, respectively. Thus, in this mode, $U_{AB} = -U_D$ and $U_{AC} = U_{dc}$. In Fig. 6(b), with the
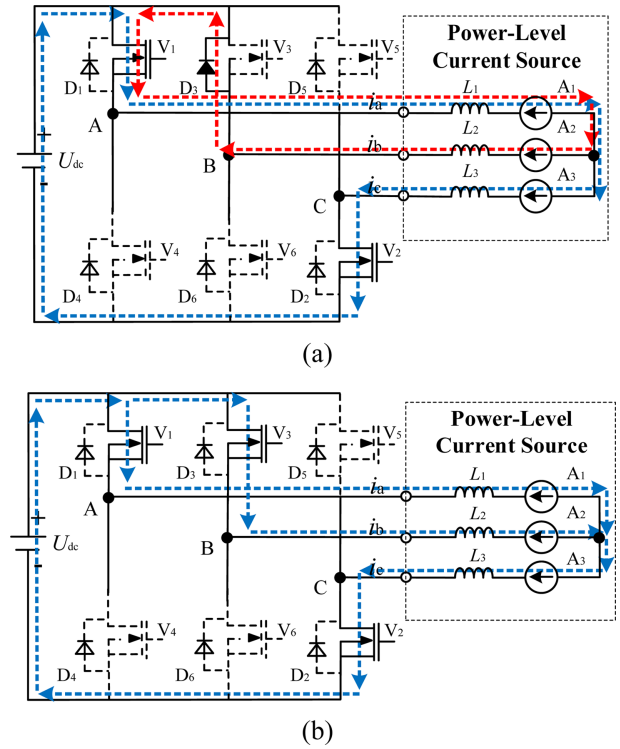

Fig. 6. (Color online) Current loops of PMSM simulator from vector U_4 to U_6. (a) Transient state. (b) Steady state.

Fig. 5. (Color online) PMSM vector control.

role of vector U_6, the current loops in steady state are $U_{dc} \rightarrow V_1 \rightarrow L_1 \rightarrow A_1 \rightarrow A_3 \rightarrow L_3 \rightarrow V_2 \rightarrow U_{dc}$ and $U_{dc} \rightarrow V_3 \rightarrow L_2 \rightarrow A_2 \rightarrow A_3 \rightarrow L_3 \rightarrow V_2 \rightarrow U_{dc}$, respectively. Thus, in this mode, $U_{AB} = 0$ and $U_{AC} = U_{dc}$.

Based on the above analysis about vectors U_4 and U_6, the relationship between phase current and line voltage about all six vectors can be obtained, which will be used to calculate the phase current commands in the PMSM numerical model.

4. Simulation and Experimental Results

To verify the feasibility of the proposed method, the universal PHIL simulator is implemented, which is shown in Fig. 7. The simulator mainly consists of a general processor of TMS320F28377S, a power-level current source, a voltage measurement unit, a virtual resolver simulation unit, a virtual Hall sensors isolation transform unit. The power-level current source in the simulator is connected to the motor driver by the inductance. The virtual motor parameters for the simulator are shown in Table 1. Furthermore, the BLDCM and PMSM Simulink models are shown in Fig. 8, and the MATLAB simulation results based on the models can be used to verify the effectiveness of the PHIL simulator.

Fig. 9 shows the back EMF, phase current and hall signal waveforms of the BLDCM simulator. The sinusoidal back EMFs e_a, e_b and the corresponding square wave currents i_a, i_b are symmetric, the six intervals from S_1 to

Table 1. Parameters of virtual motor.

Parameters	Value (BLDCM)	Value (PMSM)
Phase winding inductance	0.2 mH	–
Phase winding resistance	0.2 Ω	0.2 Ω
d axis inductances	–	1.2 mH
q axis inductances	–	1.2 mH
Number of pole pairs	1	1
Number of phases	3	3
Shape of back EMF	sinusoidal	sinusoidal

S_6 in one control period are determined by the three virtual hall sensor signals h_a, h_b and h_c. Moreover, the current relationships are, respectively, $i_a > 0$ and $i_b < 0$ in interval S_1, $i_a < 0$ and $i_b > 0$ in interval S_4. The results show that the rotor position, numerical model and control method in the BLDCM simulator are correct.

Fig. 10 shows the phase current comparison of BLDCM between the PHIL simulator and MATLAB simulation. Both tests are under the six-step commutation control mode as shown in Fig. 2, and the reference value of phase current is 2A. The MATLAB simulation current in Fig. 10(b) is similar to the simulator current in Fig. 10(a) in both steady state and transient state, which shows that the PHIL simulator can effectively realize the current control for the virtual BLDCM.

Fig. 11 shows the phase current comparison of PMSM between the PHIL simulator and MATLAB simulation. Both tests are under the vector control method as shown
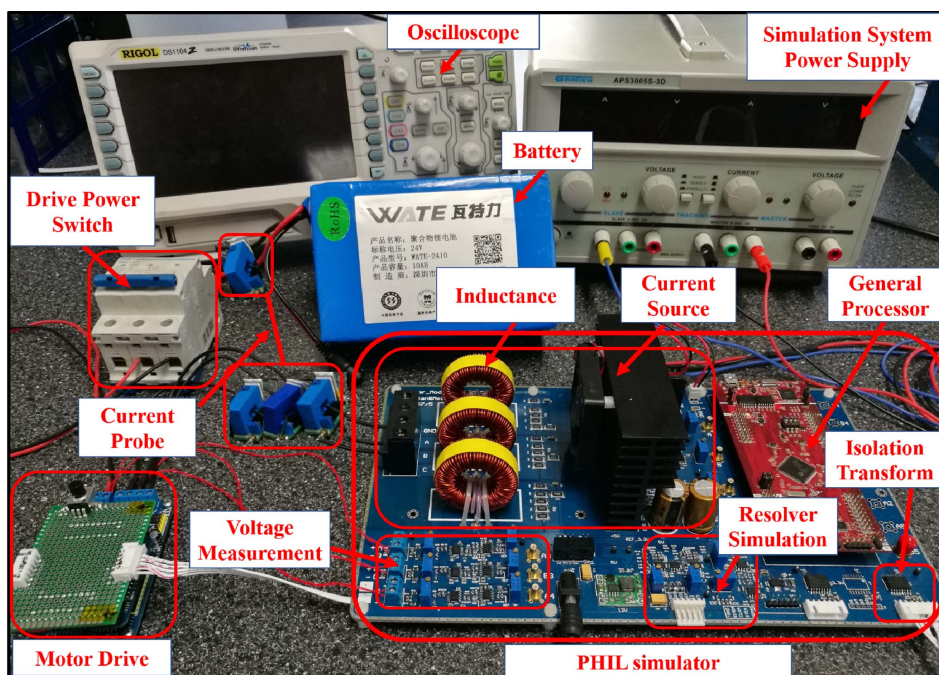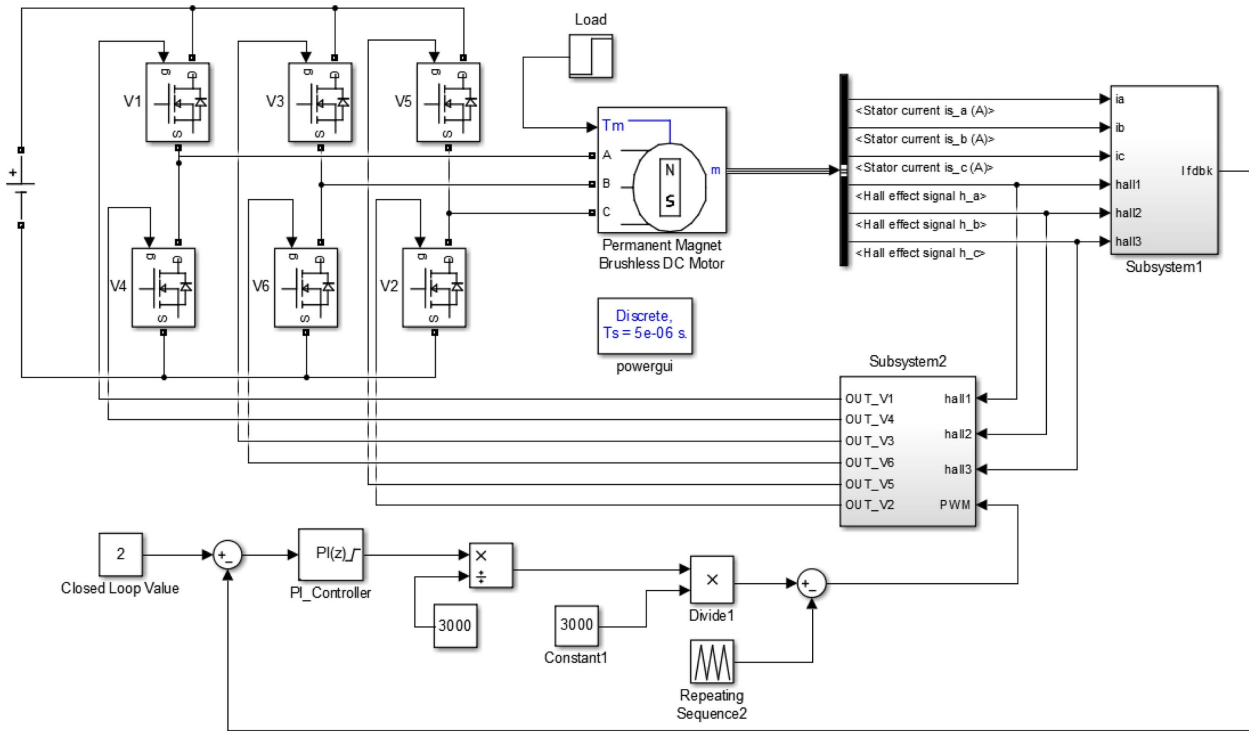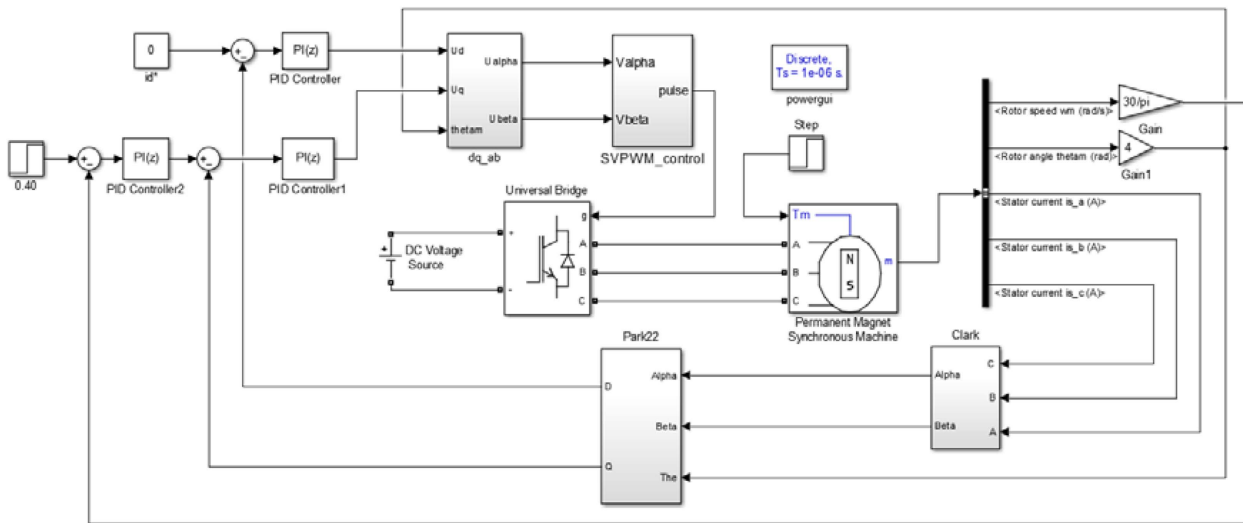

Fig. 7. (Color online) Universal PHIL simulator and motor drive.

(a)

(b)

Fig. 8. (Color online) Simulink model for MATLAB simulation. (a) BLDCM. (b) PMSM

in Fig. 5. Moreover, *d*-axis reference current is zero and *q*-axis reference current is 1.5A. The sinusoidal current in the MATLAB simulation in Fig. 11(b) is same as that of the PHIL simulator in Fig. 11(a), which proves that the current control for the virtual PMSM can be effectively realized based on the universal simulator.

Fig. 12(a) shows the actual BLDCM controlled by the same driver as that in the PHIL simulator test. The

BLDCM with sinusoidal back EMF can be regarded as the PMSM when the vector control method is used. The motor parameters are shown in Table 1. The phase current of the actual BLDCM with six-step commutation control mode is shown in Fig. 12(b), which is similar to the simulated virtual BLDCM phase current in Fig. 10. Fig. 12(c) is the phase current of the actual PMSM with vector control method, which is similar to the simulated virtual
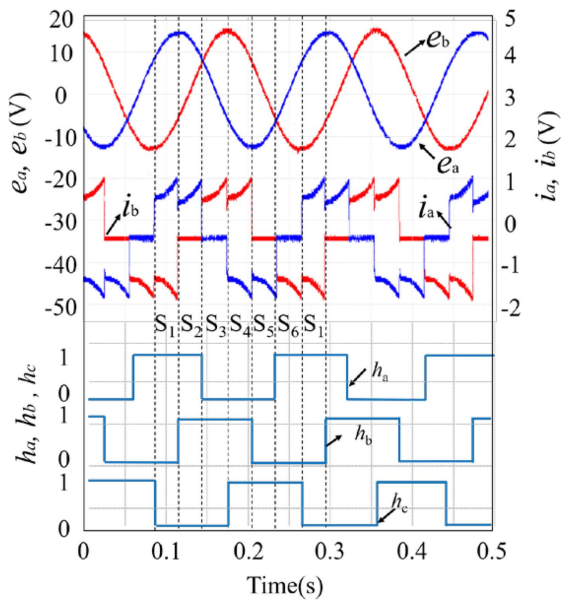
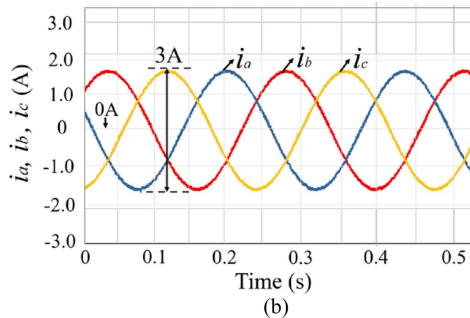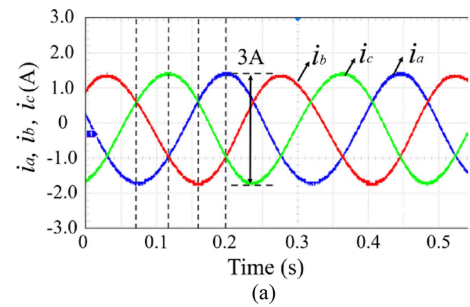**Fig. 9.** (Color online) Back EMF, phase current and hall signal waveforms of BLDCM simulator.
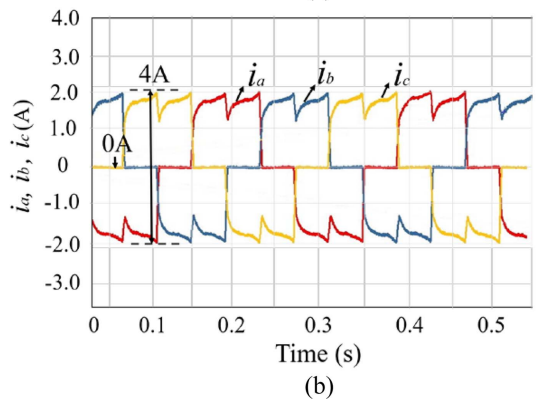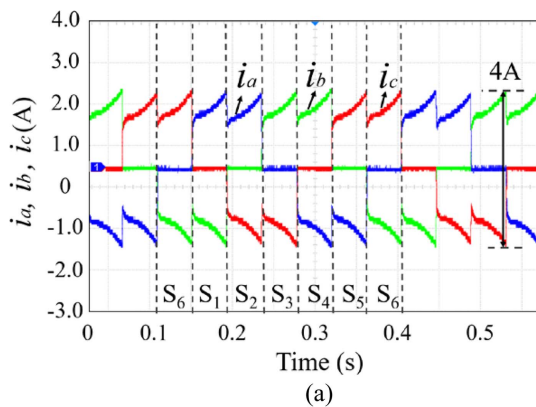

Fig. 10. (Color online) Phase current waveforms of BLDCM. (a) PHIL simulator. (b) MATLAB simulation.

PMSM phase current in Fig. 11. The experimental results prove that the universal PHIL simulator is appropriate for both BLDCM and PMSM.
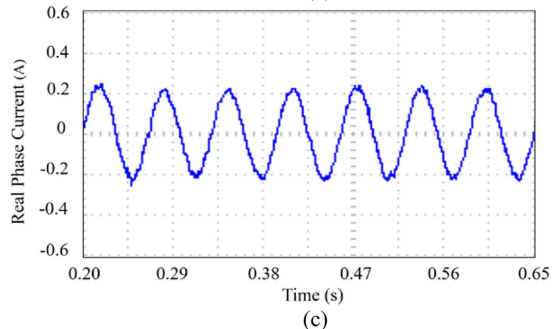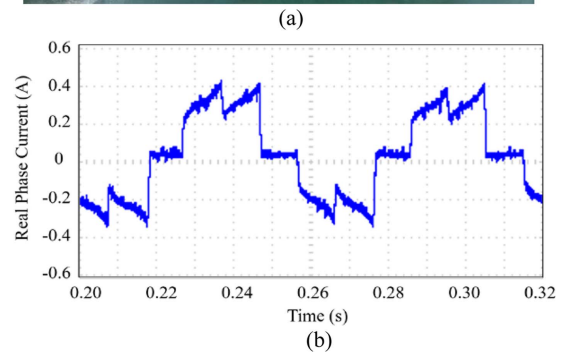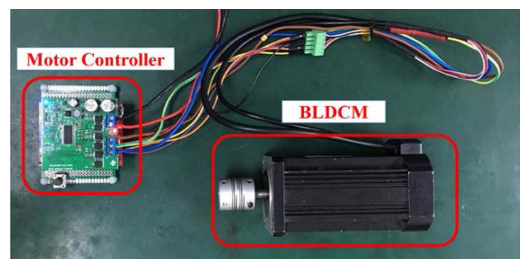

Fig. 11. (Color online) Phase current waveforms of PMSM. (a) PHIL simulator. (b) MATLAB simulation.

Fig. 12. (Color online) Actual motor and phase current waveforms. (a) Actual motor connected to controller. (b) Phase current of BLDCM. (c) Phase current of PMSM.

5. Conclusions

This paper presents a novel method to design a universal PHIL simulator for BLDCM and PMSM. The proposed simulator has the ability to acquire line voltage from the motor driver without a neutral point. The bilinear transform and inverse Z-transform based numerical model can cost low computational effort, and the simulator can be realized with one DSP. Without changing any hardware structure of the motor driver, both BLDCM and PMSM can be simulated conveniently at the power level only based on the different numerical models in the simulator. With the advantages of high efficiency and low cost, the simulator is applicable to the motor driver test and control algorithm verification for BLDCM and PMSM.

Acknowledgment

References

[1] C. L. Xia, H. W. Fang, Transactions of China Electrotechnical Society **127**, 3 (2012).

[2] F. Alvarez-Gonzalez, A. Griffo, B. Sen, and J. B. Wang, IEEE Trans. Ind. Electron. **64**, 9 (2017).

[3] N. R. Tavana and V. Dinavahi, IEEE Trans. Ind. Electron. **62**, 4 (2015).

[4] A. Hasanzadeh, C. S. Edrington, N. Stroupe, and T. Bevis, IEEE Trans. Ind. Electron. **61**, 6 (2014).

[5] J. Gao, Q. X. Xu, and Z. H. Dong, Electric Machines and Control. **22**, 4 (2018).

[6] T. Schulte and J. Bracker, in Power Electronics, Electrical Drives, Automation and Motion, Int. Conf. (2008), pp. 2195-2200.

[7] T. Schulte and J. Bracker, in Advances in Automotive Control, Int. Conf. (2010), pp. 437-442.